



The CO₂ integral emission by the megacity of St. Petersburg as quantified from ground-based FTIR measurements combined with dispersion modelling

5 Dmitry V. Ionov¹, Maria V. Makarova¹, Frank Hase², Stefani C. Foka¹, Vladimir S. Kostsov¹, Carlos Alberti², Thomas Blumenstock², Thorsten Warneke³, Yana A. Virolainen¹

¹ Department of Atmospheric Physics, Faculty of Physics, St. Petersburg State University, Russia

² Karlsruhe Institute of Technology (KIT), Institute of Meteorology and Climate Research (IMK-ASF), Karlsruhe, Germany

³ University of Bremen, Germany

10 *Correspondence to:* Dmitry V. Ionov (d.ionov@spbu.ru), Frank Hase (Frank.Hase@kit.edu) and Maria V. Makarova (m.makarova@spbu.ru)

Abstract. The anthropogenic impact is a major factor of the climate change which is highest in industrial regions and modern megacities. Megacities are a significant source of emissions of various substances into the atmosphere, including CO₂ which is the most important anthropogenic greenhouse gas. In 2019 and 2020, the mobile experiment EMME (Emission Monitoring Mobile Experiment) was carried out on the territory of St. Petersburg which is the second largest industrial city
15 in Russia with a population of more than 5 million people. In 2020, several measurement data sets were obtained during the lockdown period caused by the COVID-19 (COroNaVIrus Disease of 2019) pandemic. One of the goals of EMME was to evaluate the CO₂ emission from the St. Petersburg agglomeration. Previously, the CO₂ area flux has been obtained from the data of the EMME-2019 experiment using the mass balance approach. The value of the CO₂ area flux for St. Petersburg has been estimated as 89±28 kt km⁻² yr⁻¹ which is three times higher than the corresponding value reported in the official
20 municipal inventory. The present study is focused on the derivation of the integral CO₂ emission from St. Petersburg by coupling the results of the EMME observational campaigns of 2019 and 2020 and the HYSPLIT (HYbrid Single-Particle Lagrangian Integrated Trajectories) model. The ODIAC (Open-source Data Inventory for Anthropogenic CO₂) database is used as the source of the a priori information on the CO₂ emissions for the territory of St. Petersburg. The most important finding of the present study based on the analysis of two observational campaigns is a significantly higher CO₂ emission
25 from the megacity of St. Petersburg as compared to the data of municipal inventory: ~75800±5400 kt yr⁻¹ for 2019, ~68400±7100 kt yr⁻¹ for 2020 (~70000±16000 kt yr⁻¹ during the lockdown) versus ~30000 kt yr⁻¹ reported by official inventory. The comparison of the CO₂ emissions obtained during the COVID-19 lockdown period in 2020 to the results obtained during the same period of 2019 demonstrated the decrease in emission of 8% or 5800 kt yr⁻¹.

Keywords: ground-based remote sensing, portable spectrometers, FTIR spectroscopy, mobile experiments, anthropogenic
30 emissions in megacities, transport modelling of air pollutants, CO₂, ODIAC, HYSPLIT



1 Introduction

Accurate quantitative assessment of anthropogenic emissions into the atmosphere is necessary for studying the mechanisms and factors that determine the impact of changes in atmospheric composition on climate, ecosystems and human health. Also, such an assessment is important for the development and control of compliance of the national policies in the field of environmental and climate protection to international agreements, regulations and standards (Pacala et al., 2010; Ciais et al., 2015; UNFCCC, 2015). In 2018, World Meteorological Organisation (WMO) established the IG3IS division (Integrated Global Greenhouse Gas Information System). Its activities are related to international efforts relevant to the implementation of the Paris Agreement under the United Nations Framework Convention on Climate Change (UNFCCC, 2015). The main goal of IG3IS is “to expand the observational capacity for greenhouse gases (GHG), extend it to the regional and urban domains, and develop the information systems and modelling frameworks to provide information about GHG emissions to society” (IG3IS, 2020).

According to statistics for 2018, 4.2 billion people or about 55% of the World's population live in cities. Urban areas are responsible for more than 70% of global energy-related CO₂ emissions (Canadell et al., 2010). Total CO₂ emissions by developed countries can be estimated with good accuracy on the basis of the total consumption of fossil fuel (FF). At the same time, available data on regional and local emissions have a significantly lower level of confidence (Ciais et al., 2015; Bréon et al., 2015; Kuhlmann et al., 2019). Usually, to check the accuracy of the CO₂ emission inventories (the so-called “bottom-up” data), the independent “top-down” approach is applied which is based on a combination of atmospheric observations and numerical simulations. Currently, the efforts in this direction are being made by international scientific communities in the framework of such large-scale projects as, for example, the VERIFY project (<https://verify.lsce.ipsl.fr/>) and the CO₂ Human Emissions (CHE) project (<https://www.che-project.eu/>). As an example of successful implementation of the “top-down” approach one can mention the experience of the United Kingdom in the evaluation of greenhouse gas emission national inventory (Stanley et al., 2018; WMO Greenhouse Gas Bulletin, 2018). Disaggregation of national FF CO₂ emission estimates provided the possibility to compile ODIAC (Open-source Data Inventory for Anthropogenic CO₂) which is a high resolution global open database of anthropogenic CO₂ emissions (Oda and Maksyutov, 2011; Oda et al. 2018).

Recently, much attention has been paid to the improvement of the estimates of the CO₂ emissions by the world's largest megacities (Mays et al., 2009; Wunch et al., 2009; Bergeron and Strachan, 2011; Levin et al., 2011; Silva et al., 2013; Hase et al., 2015; Vogel et al., 2019; Babenhauserheide et al., 2020). A lot of studies are based on the results of routine observations by the international ground-based monitoring networks: ICOS (ICOS, 2020), NOAA ESRL (NOAA ESRL, 2020), TCCON (TCCON, 2020), COCCON (COCCON, 2020), FLUXNET (FLUXNET, 2020). Also, national instrumental air quality control systems were used (Airparif, 2020) as well as the satellite measurement systems (Kuhlmann et al., 2019, Oda et al. 2018) and individual observational stations (Zinchenko et al., 2002; Pillai et al., 2011). It is important to mention measurement campaigns organized in the framework of major scientific projects, such as InFLUX (sites.psu.edu/influx;



Turnbull et al., 2014), Megacities Carbon Project (<https://megacities.jpl.nasa.gov/portal/>; Duren and Miller, 2012), MEGAPOLI (<http://www.megapoli.info>, Lopez et al., 2013), CO₂-Megapolis project in Paris (<https://co2-megapolis.lscce.ipsl.fr>, Bréon et al., 2015), COCCON – Paris (<http://www.chasing-greenhouse-gases.org/coccon-in-paris/>), and VERIFY (<https://verify.lscce.ipsl.fr/>). The important goal is to improve existing techniques and to develop new algorithms for the space-borne detection of the CO₂ plumes originating from intensive compact sources such as large cities and big thermal power plants (TPP) (Kuhlmann et al., 2019; SMARTCARB project, <https://www.empa.ch/web/s503/smartcarb>). Bovensmann et al. (2010) and Pillai et al. (2016) proposed to create and launch new specialised satellite instruments for studying natural and anthropogenic sources and sinks of carbon dioxide with high spatial resolution. At the same time, the variety of modelling tools used to simulate the atmospheric CO₂ fields and assimilate the results of observations is also quite large: ranging from simple mass balance models (Hiller et al., 2014; Zimnoch et al., 2010, Makarova et al., 2018) to modern transport and photochemical models (Ahmadov et al., 2009; Göckede et al., 2010, Pillai et al., 2011, Pillai et al., 2012).

The present study is focused on the CO₂ emission by St. Petersburg, Russian Federation. The area of St. Petersburg urban agglomeration is about 1440 km², while the city centre characterized by high construction density occupies 650 km². The city has a population of ~5.4 million people (the official data for 2018, https://en.wikipedia.org/wiki/Saint_Petersburg); according to unofficial data the population is now more than 7 million. The population density is ~3800 people/km² on average. It can reach ~7300 people/km² on the territories with high construction density (Solodilov, 2005). The data on total emissions of anthropogenic air pollutants in St. Petersburg are provided in the annual reports of the municipal Environmental Committee (Serebriksky, 2018; Serebriksky, 2019). Published data are based on the emission sources inventory method ("bottom-up") where CO₂ fluxes for urban areas are calculated on the basis of information about the landscape and the type of anthropogenic activity (e.g., number and type of buildings, location of roads, traffic intensity, the presence and type of TPP, etc.) using appropriate emission factors (Gurney et al., 2002; Serebriksky, 2018). On average, the contribution of St. Petersburg to the total greenhouse gas emissions of the Russian Federation is about 1%. According to official inventory data for 2015, the integral CO₂ emission from the territory of St. Petersburg is about 30 Mt/year and the inter-annual variability of this estimate in the period 2011-2015 did not exceed 1 Mt/year (Serebriksky, 2018). More than 90% of the St. Petersburg emissions are related to power production, while the remaining 10% are related to industry, agriculture, household and industrial waste. These data differ, for example, from the results obtained in the study of the structure of anthropogenic CO₂ emissions by the city of Baltimore (Maryland, USA): Roest et al. (2020) have reported that electricity production in Baltimore emits only 9% of CO₂ and the main part of emissions is related to transport (automobile 34%, marine 4%, air and rail transport 2%), as well as to the commercial sector (20%), industry (19%) and private residential housing (12%).



95 The main anthropogenic source of CO₂ is associated with the consumption of fossil fuels. However, a number of
studies have demonstrated that for the territories with high population density carbon dioxide produced by human respiration
process can make a significant contribution to total emissions (Bréon et al., 2015; Ciais et al., 2007; Widory and Javoy,
2003). According to some estimates, one person emits by breathing on average 1 kg of CO₂ per day (Prairie and Duarte,
2007), which would amount to about 3 Mt of CO₂ per year for St. Petersburg. Bréon et al. (2015) have shown that for Paris
the CO₂ emission from human breathing constitutes 8% of the total inventory emissions of the metropolis due to the use of
100 fossil fuels. So, the official inventory ("bottom-up") estimates of the CO₂ emissions for St. Petersburg (Serebriisky, 2018)
may have significant uncertainties both in the estimates of integral emissions and in the data on the spatial and temporal
distribution of the CO₂ fluxes. This suggestion is confirmed by the significantly different values of the CO-to-CO₂ emission
ratio (ER) for St. Petersburg obtained by Makarova et al. (2020) from the field measurements (ERCO/CO₂ ≈ 6 ppbv/ppmv)
and calculated using the official emission inventory data reported by Serebriisky (2018) (ERCO/CO₂ ≈ 21 ppbv/ppmv).

105 In 2019, the mobile experiment EMME (Emission Monitoring Mobile Experiment) was carried out on the territory of
the St. Petersburg agglomeration with the aim to estimate the emission intensity of greenhouse (CO₂, CH₄) and reactive (CO,
NO_x) gases for St. Petersburg (Makarova et al., 2020). St. Petersburg State University (Russia), Karlsruhe Institute of
Technology (Germany) and the University of Bremen (Germany) jointly prepared and conducted this city campaign. The
core instruments of the campaign were two portable FTIR (Fourier Transform InfraRed) spectrometers Bruker EM27/SUN
110 which were used for ground-based remote sensing measurements of the total column amount of CO₂, CH₄ and CO at upwind
and downwind locations on opposite sides of the city. The applicability and efficiency of this measurement scenario and
EM27/SUN spectrometers have been shown by Hase et al., 2015, Chen et al., 2016; Dietrich et al., 2020. The description of
the EMME experiment has been given in full detail in the paper by Makarova et al. (2020). This study has also reported the
estimations of the area fluxes for the emissions of CO₂, CH₄, NO_x and CO by St. Petersburg. In 2020, the EMME experiment
115 was continued. It started in March before the COVID-19 pandemic lockdown and consisted of six days of field
measurements (three days before the lockdown and three days during the lockdown).

The present study continues the analysis of the data of EMME-2019 and demonstrates the first results of the 2020
campaign. As stated above, we concentrate our efforts only on the CO₂ emissions leaving the results relevant to other gases
beyond the scope of the study. It should be emphasized that:

- 120 - As an extension to the work by Makarova et al. (2020) our goal in this study is to estimate the integral CO₂ emission
by St. Petersburg megacity rather than area fluxes.
- We apply the HYSPLIT dispersion model, HYbrid Single-Particle Lagrangian Integrated Trajectories (Draxler and
Hess, 1998; Stein et al., 2015) while the first results of the EMME-2019 campaign were obtained with the help of a box
model.
- 125 - For model simulations, we use the ODIAC database (Oda and Maksyutov, 2011) as the a priori information on the
spatial and temporal distribution of anthropogenic CO₂ emissions for the territory of St. Petersburg.



- In addition to the EMME-2019/2020 field campaign data we also use the results of routine in-situ measurements of local CO₂ concentrations (Foka et al., 2019).

130 **2 The EMME measurement campaign (short summary)**

The main goal of the EMME measurement campaigns in 2019 and 2020 organized jointly by SPbU (St. Petersburg State University, Russia), KIT (Karlsruhe Institute of Technology, Germany) and UoB (University of Bremen, Germany) was to evaluate emissions of CO₂, CH₄, CO and NO_x from the territory of St. Petersburg. Similar to 2019, the EMME-2020 campaign was conducted in spring (March - early May). This time of the year is preferable for a successful study of urban emissions, especially CO₂, due to the following reasons: (1) a daylight duration is sufficient for FTIR remote sensing measurements; (2) the influence of vegetation processes on the daily evolution of the CO₂ concentration in the atmosphere is negligible; (3) the winter heating of the city buildings is still active which is a significant source of the CO₂ emissions for northern cities such as St. Petersburg. In contrast to the 2019 campaign, when two mobile EM27/SUN FTIR spectrometers were used in the field experiment for simultaneous measurements inside and outside of the air pollution plume, all measurements in 2020 were performed with only one spectrometer which was transported between clean and polluted locations within one day. In 2019, the field measurements were carried out during 11 days in total, and on 6 days in 2020. The number of observations in 2020 was smaller than in 2019 due to the quarantine restrictions related to the COVID-19 pandemic. These restrictions were imposed in St. Petersburg on 28 March, 2020. During several days of the 2020 campaign, measurements inside the city pollution plume were made at two locations, which allowed to increase the total number of observations.

A number of studies (Pillai et al., 2016; Broquet et al. 2018; Kuhlmann et al., 2019; Babenhauerheide et al., 2020) have shown that emissions from large CO₂ sources (cities, thermal power plants) can be characterized by the difference between the results of measurements of the carbon dioxide concentration in the dry atmospheric column inside and outside of the pollution plume (ΔXCO_2). The results of measurement campaigns in 2019 and 2020 have shown that for St. Petersburg $\Delta XCO_2=0.05\text{...}4.46$ ppmv. For comparison, similar studies revealed the following values of ΔXCO_2 : 0.16...1.03 ppmv for Berlin, Germany (Kuhlmann et al., 2019), 0.80...1.35 ppmv for Paris, France (Pillai et al., 2016; Broquet et al. 2018), and 0...2 ppmv for Tokyo, Japan (Babenhauerheide et al., 2020). So, for St. Petersburg, the highest values of ΔXCO_2 were detected (4.46 ppmv), if compared to similar measurements in Berlin, Paris and Tokyo. It should be noted that the value of ΔXCO_2 depends not only on the integral emission of the source, but also on its type (point, linear or area), the geometry of the field experiment and on the meteorological situation during the measurements.



3 Modelling of anthropogenic air pollution

3.1 A priori data on FF CO₂ emissions (ODIAC)

The global emission inventory ODIAC (Oda and Maksyutov, 2011; Oda, Maksyutov and Andres, 2018) is used in the present study for characterisation of the area fluxes of the CO₂ emission from the territory of St. Petersburg and its suburbs. ODIAC provides global information on monthly average CO₂ emissions due to consumption of fossil fuels. The high spatial resolution of ODIAC (1 km × 1 km) is achieved through a joint interpretation of the existing global inventory of anthropogenic CO₂ sources, data on FF consumption, and satellite observations of the night-time glow of densely populated areas of the Earth. We use the data for 2018 emissions given in the ODIAC2019 version (Oda and Maksyutov, 2020).

The CO₂ emission data have been extracted from the ODIAC database for the domain that includes St. Petersburg and its suburbs (59.60-60.29° N, 29.05-31.33° E, Fig. 1). The sources of anthropogenic CO₂ emissions are concentrated within the administrative borders of the city. Most of these sources have intensities of ~4000 tons/month/km² and higher and are located within the borders of the city ring road. Summing up the ODIAC data within the city borders gives an estimate of the average integrated CO₂ emission of ~2710 kt per month with variations from 2429 kt in July to 3119 kt in March (Fig. 2). The emissions are maximal in late winter and early spring, and are minimal in summer. In general, the seasonal variability of emissions is insignificant (~8%), therefore the data for 12 months of 2018 were averaged in order to obtain an estimate of the mean annual distribution of urban CO₂ emissions. The integrated annual emission of St. Petersburg equals to 32529 kt, which is in good agreement with published official estimates: about 30 million tons for the period from 2011 to 2015 (Serebriksky, 2018).

The nominal latitude/longitude size of the ODIAC data pixel is 30 arcseconds (Oda and Maksyutov, 2011), which for St. Petersburg corresponds to an area of 0.93 km × 0.46 km (0.43 km²). It should be noted that the average annual urban emission flux is ~26 kt km⁻² while in the central part of the city it can reach up to 80 kt km⁻². There is one pixel in the ODIAC data located in the centre of St. Petersburg with an extremely high emission flux of 7000 kt km⁻². Since such a high CO₂ emission at a particular location seems to be an outlier, this value was deleted and replaced by the value averaged over the neighboring ODIAC pixels. As a result, it amounted to 42 kt km⁻².

3.2 HYSPLIT model general setup

The spatial and temporal evolution of the urban pollution plume was simulated using the HYSPLIT model (Draxler and Hess, 1998; Stein et al., 2015). Calculations were performed for the territory of the St. Petersburg agglomeration using the offline version of the HYSPLIT model with the setup similar to the one that was successfully used previously for the NO_x plume modelling (Ionov and Poberovskii, 2019; Makarova et al., 2020). A 3-dimensional field of anthropogenic air pollution was calculated for a spatial domain with coordinates 54.8°-61.6° N, 23.7°-37.8° E; the domain grid size is



0.05°×0.05° latitude and longitude (see Fig. 3, top). The vertical grid of the model is set to 10 layers with the altitude of the upper level at 1, 25, 50, 100, 150, 250, 350, 500, 1000 and 1500 meters a.s.l., respectively. As a source of meteorological information (vertical profiles of the horizontal and vertical wind components, temperature and pressure profiles, etc.), the NCEP GDAS (National Centers for Environmental Prediction Global Forecast System) data were used, presented on a global spatial grid of 0.5° × 0.5° latitude and longitude with time interval of 3 hours (NCEP GDAS, 2020). Spatial distribution of FF CO₂ emission sources and their intensities are taken from the ODIAC database. The original ODIAC data were converted into a set of larger pixels (~1 km²). Pixels with the area fluxes lower than 8 kt km⁻² have been filtered out in order to keep only the urban sources which could be attributed to the St. Petersburg agglomeration. The resulting array which was used as the input for HYSPLIT consisted of 376 pixels and is shown in Fig. 3 (bottom). The integral CO₂ emission that corresponds to this array equals to 26316 kt year⁻¹; this is the value being used as a HYSPLIT first guess hereafter.

3.3 Simulations of ground-level CO₂ concentrations

Routine measurements of CO₂ surface concentrations have been carried out at the atmospheric monitoring station of St. Petersburg University in Peterhof (59.88° N, 29.82° E) since 2013. These observations are the in situ measurements using a gas analyzer Los Gatos Research GGA 24r-EP. The instrument is installed on the outskirts of a small town of Peterhof in the suburbs of St. Petersburg (see location in Fig. 1). This place is far enough away from busy streets and other local sources of pollution, with an ambient air intake being 3 meters above the surface. To test the HYSPLIT model setup for the St. Petersburg region, we calculated the surface concentration of CO₂ near the Peterhof during the 2019 EMME measurement campaign – from March 20 to April 30, 2019 (Makarova et al., 2020). The results of the model calculations were compared to the data of in situ measurements (due to the instrument failure in 2020 the comparison is limited to the period of EMME campaign in 2019 only). Observational data and simulation results were averaged over 3-hour intervals. The resulting comparison is shown in Fig. 4. The model reproduces the temporal variations of CO₂ including the main periods of significant growth of concentration; the correlation coefficient between the calculation and measurements is equal to 0.72. The background value of the surface concentration is taken as 415 ppmv based on long-term local measurements. It is important to emphasize that quantitative agreement is achieved by linear scaling of the a priori integral urban CO₂ emission. The scaling coefficient for emissions corresponds to the value of the integral urban CO₂ emission from the territory of St. Petersburg of 44800±1900 kt year⁻¹ (the given uncertainty is due to the uncertainty of the fitted scaling factor). This value is noticeably higher than official estimates mentioned above and ODIAC data for 2018 (32529 kt). The average discrepancy between the measurement and simulation data shown in Fig. 4 is 2±9 ppmv (model calculations are systematically lower).



4 Evaluation of integrated CO₂ emissions from field FTIR measurements

4.1 The results of the EMME-2019 campaign

We simulated the CO₂ total column (TC) for the time periods and locations of FTIR mobile measurements conducted in the framework of the EMME-2019 experiment in March-April 2019 (Makarova et al., 2020). Obviously, the anthropogenic contribution to the CO₂ TC is concentrated mostly in the lower boundary layer, with a top height of ~200 to ~1600 m. Therefore, HYSPLIT model was configured to simulate CO₂ concentrations at 10 altitude levels (0-1500 m), which were then integrated to obtain the CO₂ column in the boundary layer. The differences between the results of FTIR measurements of the CO₂ TC inside and outside the pollution plume (ΔCO_2) were compared with the differences in the CO₂ column in the boundary layer simulated by HYSPLIT at the corresponding locations. HYSPLIT calculations were performed with a temporal resolution of 15 minutes. For the sake of comparison, the simulation results and measurement data were averaged over time periods of field observations.

In order to obtain a quantitative agreement between simulated and observed ΔCO_2 , the input inventory data (the ODIAC data) should be scaled (Flesch et al., 2004). The scaling factor was derived as follows. The data from all days of measurements were considered together with corresponding model simulations, see Fig.5a as an example of a scatter plot. The scaling factor is determined as a slope value of the regression line (e.g. the slope is 2.88 ± 0.21 , as shown in Fig.5a).

The error assessment for the scaling factor should be discussed in some detail. The 1σ precision for the XCO₂ individual measurement is of the order of 0.01 %–0.02 % (<0.08 ppm) (e.g. Gisi et al., 2012; Chen et al., 2016; Hedelius et al., 2016; Klappenbach et al., 2015; Vogel et al., 2019). The error of the scaling factor was estimated under the assumption that the measurement errors are the same for all days as well as the model simulation errors. The error bars indicated in Fig. 5a as boxes are in fact the variations of ΔCO_2 obtained as standard deviation of observations and simulations within one observational series. Obviously, these quantities comprise both measurement errors and temporal variability of the CO₂ TC. One can see that these quantities differ from day to day.

Fig. 5b demonstrates that the model reproduces well the evolution of ΔCO_2 recorded in field measurements; the correlation coefficient between the results of modelling and observations is 0.94. The derived scaling factor yields the integral anthropogenic CO₂ emission value of 75800 ± 5400 kt year⁻¹; e.g. the value of 75800 results from the multiplication 26316×2.88 (the 2.88 here is the slope in Fig.5a, and 26316 is the model first guess, see 3.2). Resulting CO₂ emission rate is almost twice as high as the above estimate, based on the analysis of ground-level CO₂ measurement data (Section 3.3, 44800 ± 1900 kt year⁻¹). This difference may indicate a significant contribution of elevated CO₂ sources (industrial chimneys) that could not be registered by the ground-level in situ measurements, as the elevated exhausts of pollution are more likely to further rise up, rather than descend to the ground. In contrast, FTIR measurements of the total column keep being sensitive to this kind of emissions. In addition, while FTIR measurements implement a "cross section" of the urban pollution emission



zone in a series of multidirectional trajectories (depending on the wind direction), local ground-level in situ measurements at a specific location (Peterhof) can not capture the contribution of the entire mass of urban emissions. Thus, estimates of integral CO₂ emissions based on the interpretation of ground-level measurements in Peterhof can be considered as a lower limit of an estimate.

The previously accomplished analysis of the results of EMME-2019 included, in particular, derivation of the area fluxes of urban CO₂ emissions on the trajectories corresponding to the movement of air mass between locations on the downwind and upwind sides of the megacity. The obtained mean value of the CO₂ area flux was equal to 89±28 kt yr⁻¹ km⁻² and was attributed to the emission from the city centre (Makarova et al., 2020). As shown above, in the current study, the application of the HYSPLIT model allowed us to estimate the integral anthropogenic CO₂ emission of the entire megacity. In order to check the consistency with previous results, in the present study we made calculations of area fluxes on the air trajectories of field measurements using the ODIAC emission database scaled to the integral CO₂ emission derived from the results of EMME-2019 combined with the HYSPLIT simulations (75800±5400 kt year⁻¹). Schematically, the air trajectories corresponding to the 2019 FTIR measurement locations are shown in Fig. 6. These trajectories were simulated as backward trajectories by the HYSPLIT model in the boundary layer of the atmosphere. The resulting values of anthropogenic CO₂ area fluxes calculated by integrating the ODIAC data along the trajectories presented in Fig. 6, are shown in Fig. 7 in comparison with the experimental estimates by Makarova et al., 2020. As in the study by Makarova et al., 2020, the width of the air paths was assumed to be 10 km. On average, according to ODIAC data, the area flux for the 2019 measurement trajectories was 106±9 kt yr⁻¹ km⁻², that is somewhat higher than the experimental estimates (89±28 kt yr⁻¹ km⁻²) but agree within the error limits. Significantly higher variability in the experimental data may be related to the variability of the wind field, which is not taken into account in the simplified mass balance approach.

4.2 The results of EMME-2020 and comparison with EMME-2019

The data of mobile FTIR measurements performed in March-April 2020 were processed and analysed in the same way as it was done for data acquired during the measurement campaign in 2019. The comparison of the observed and simulated mean values of ΔCO₂ is shown in Fig. 8. Similar to the results of 2019, the HYSPLIT simulations reproduce well the observed evolution of ΔCO₂. The correlation coefficient between the simulations and observations is 0.78. The estimation of the CO₂ emission was done using the described above approach based on scaling the ODIAC data. For the EMME-2020, the derived integral anthropogenic CO₂ emission is 68400±7100 kt yr⁻¹, which is about 10% lower than the estimate obtained for 2019 (75800±5400 kt yr⁻¹).

It should be noted that one can expect lower anthropogenic CO₂ emissions in the 2020 measurement data compared to the same period in 2019, since restrictive measures were imposed in St. Petersburg on March 28 due to the COVID-2019 pandemic. A number of studies have already reported significant reductions of air pollution that followed the lockdown



events in different regions of the world (see e.g. Petetin et al., 2020; Pathakoti et al., 2020; Koukouli et al., 2020). According to Yandex data (<https://yandex.ru/covid19/stat>) the traffic intensity in the city of St. Petersburg decreased to 12-26% of the usual value on weekdays in the first week of quarantine (from March 30 to April 3) and amounted to 28-33% in the following week (from April 6 to April 10). Since we have no official data on the CO₂ emissions by traffic at our disposal, we used the average estimate for European countries, according to which the contribution of traffic to total emission constitutes 30% (European Parliament News, 2020). Under this assumption, a reduction in traffic activity down to 30% of the normal level should result in a reduction in total anthropogenic CO₂ emissions by 21% $((1.0-(0.7+0.3\times 0.3))\times 100\%)$. The estimated integrated CO₂ emission derived from the 2020 measurements is $\sim 68400 \pm 7100 \text{ kt yr}^{-1}$. If we exclude from the scaling factor calculation the results of measurements performed before the start of the quarantine, than for the integrated emission we obtain $\sim 70000 \pm 16000 \text{ kt yr}^{-1}$. The comparison with the same period of 2019 ($\sim 75800 \pm 5400 \text{ kt yr}^{-1}$) gives the difference in emission of 8% or 5800 kt yr^{-1} . This difference is within the error limits of the estimates.

The weak response of urban CO₂ emissions to restrictive quarantine measures may indicate a relatively small contribution of traffic to the total CO₂ emissions from the territory of St. Petersburg. This may be due to the higher contribution of emissions associated with residential heating (including consumption of natural gas in private residences, e.g. stoves and water boilers), which is more important for such a northern city as St. Petersburg, unlike many European cities. Normally, the heating is still working in St. Petersburg in March and April, and the corresponding CO₂ emissions cannot be reduced due to the quarantine. The validity of our conclusion with regard to the transport contribution is based on the high sensitivity of FTIR measurements of XCO₂ using EM27/SUN spectrometers and COCCON methodology. If the emission from traffic was higher it would have been definitely detected during the campaign. The high sensitivity of our measurements to the CO₂ pollution from different sources is demonstrated by the following examples. The results of EMME-2019 revealed that the emission of a single TPP located on the north-eastern side of the city (see Fig. 9) can add $\sim 5 \times 10^{19}$ molecules/cm² to the CO₂ TC (Makarova et al., 2020). During the 2020 measurement campaign, one of the series of FTIR measurements was performed near the Waste Processing Plant (WPP) on the eastern side of the city (see Fig. 9). The contribution of this local CO₂ source was $\sim 1 \times 10^{19}$ molecules/cm². We emphasise that these measurements, being significantly affected by local sources, were excluded from statistical analysis. However, the given examples indicate the crucial role of stationary, non-transport sources of emissions, which were not subject to restrictive quarantine measures.

A thorough analysis of all experiments performed during the 2019 and 2020 measurement campaigns has shown that there were days with similar air trajectories and similar downwind measurement locations. These situations occurred twice: on March 27, 2019 and April 5, 2020, and on April 1, 2019 and April 8, 2020 (see Fig. 9). Both series of 2020 measurements, on April 5 and April 8, were performed during the COVID-19 quarantine period. We calculated the CO₂ area fluxes for these days applying the mass balance approach which was used by Makarova et al., 2020. The results are presented in Table 1. Unexpectedly, the estimates indicate an increase of area fluxes during the quarantine period in 2020, compared to the same period in 2019. According to the data of weather archive



(http://rp5.ru/Weather_archive_in_Saint_Petersburg, last access 3 November 2020), the mean ambient temperature in St. Petersburg was +5.0 °C and +3.2 °C for the period from March 27 to April 8 in 2019 and 2020, accordingly. Thus, somewhat colder weather in 2020 may contribute to the increase of CO₂ emission due to the more intense residential heating. However, the high uncertainty of the CO₂ area flux estimates due to the uncertainties of the wind field and of the effective path length (for details, see Makarova et al., 2020) does not allow us to gain sufficient confidence in the nature of the detected differences.

To our opinion, the most important finding of our study based on the analysis of two observational campaigns is a significantly higher CO₂ emission from the megacity of St. Petersburg as compared to the data of municipal inventory: ~75800±5400 kt yr⁻¹ for 2019, ~68400±7100 kt yr⁻¹ for 2020 versus ~30000 kt yr⁻¹ reported by official inventory. Besides, this finding is consistent with the estimate of the CO₂ emission area flux by Makarova et al., 2020 which was about double of the EDGAR inventory for St. Petersburg (EDGAR, 2019). The difference can be partly explained by the impact of diurnal and seasonal variations of anthropogenic activity, since our measurements were conducted during the period of maximum CO₂ emission (early spring and afternoon) and therefore represent the upper limit of the emission estimates. According to the ODIAC data (see Fig. 2) emissions in March and April have to be scaled down by the factor of ~1.07 to represent the annual average. The global database of hourly scaling factors (Nassar et al. 2013) gives also a factor of ~1.07 for St. Petersburg to scale down the afternoon emission rates to the daily average. So, dividing our estimates twice by 1.07 gives ~59000±66000 kt yr⁻¹, which is still higher than the official inventory value. Compared to other world cities, the integral CO₂ emission of St. Petersburg is not that high – e.g. the ODIAC inventory reports: ~18000 kt yr⁻¹ for San Francisco, ~37000 kt yr⁻¹ for Paris, ~51000 kt yr⁻¹ for Mexico, ~88000 kt yr⁻¹ for Delhi, ~106000 kt yr⁻¹ for Moscow, ~136000 kt yr⁻¹ for Hong Kong, ~172000 kt yr⁻¹ for Tokyo and ~227000 kt yr⁻¹ for Shanghai (the data is taken from the paper by Umezawa et al., 2020, Fig. 3). Typically, these estimates of urban CO₂ emissions are strongly correlated with the city's population – e.g. ~1 million people at San Francisco and ~23 million people at Shanghai.

5 Summary and conclusions

In 2019 and 2020, in spring, the mobile experiment EMME (Emission Monitoring Mobile Experiment) was carried out on the territory of St. Petersburg, which is the second largest industrial city in Russia with a population of more than 5 million people. In 2020, several measurement series were obtained during the lockdown period caused by the COVID-19 pandemic. Previously, the CO₂ area flux has been obtained from the data of the EMME-2019 experiment using the mass balance approach. The present study is focused on the derivation of the integral CO₂ emission from St. Petersburg by combining the results of the EMME observational campaigns of 2019 and 2020 and the HYSPLIT model. The ODIAC database is used as the source of the a priori information on the CO₂ emissions for the territory of St. Petersburg.



The HYSPLIT model coupled with the scaled input from the ODIAC database reproduces well the results of FTIR observations of the CO₂ TC during both campaigns: the correlation coefficient between the results of modelling and observations is 0.94 for 2019 and 0.78 for 2020. Lower value of the correlation coefficient for 2020 can be partly explained by the change in the spatial distribution of the CO₂ emission sources during the COVID-19 pandemic lockdown which could differ from the ODIAC distribution of the FF CO₂ sources. However, the number of data is not sufficient to confirm this suggestion. The most important finding of the study based on the analysis of two observational campaigns is a significantly higher CO₂ emission from the megacity of St. Petersburg as compared to the data of municipal inventory: ~75800±5400 kt yr⁻¹ for 2019, ~68400±7100 kt yr⁻¹ for 2020 (~70000±16000 kt yr⁻¹ during the lockdown) versus ~30000 kt yr⁻¹ reported by official inventory. The comparison of CO₂ emissions obtained during the COVID-19 lockdown period in 2020 to the results obtained during the same period of 2019 demonstrated a decrease in emission of 8% or 5800 kt yr⁻¹.

There was an attempt to simulate the in situ measurements of the CO₂ concentration performed at the observational site located in the suburb of the St. Petersburg megacity during the two-month period (March-April 2019). In this case the correlation coefficient between model simulations and observations was 0.72. In contrast to the estimates of the CO₂ emissions from FTIR measurements presented above, the simulation of in situ measurements gives a much lower value (by a factor of 1.5-1.7) of the CO₂ integrated emission: 44800±1900 kt year⁻¹. Similar differences were previously found between estimates of the CO₂ area fluxes for the central part of St. Petersburg, obtained both from the analysis of FTIR measurements, and from in situ measurements of CO₂ concentration (Makarova et al., 2020). This fact may indicate a significant contribution of elevated CO₂ sources (industrial chimneys) that could not be registered by the ground-level in situ measurements (in contrast to FTIR measurements of the total column). The approach of monitoring the outflows of large cities using arrays of compact FTIR spectrometers seems a promising and cost-effective route for assessing and monitoring the CO₂ emissions of these important sources. Recurring campaigns performed over extended periods or even the erection of permanent observatories as demonstrated by Chen et al. (Dietrich et al., 2020) should be recognized as crucial components of strategies aiming at improved observational capacity for greenhouse gases on regional and urban domains.

365 **Data availability**

The datasets containing the EM27/SUN measurements during EMME-2019 and EMME-2020 can be provided upon request; please contact Maria Makarova (m.makarova@spbu.ru) and Frank Hase (Frank.Hase@kit.edu)

Author contributions

DVI and MVM conceived the study. MVM, DVI, FH, CA, VSK, SCF contributed greatly to the experimental part of the study. SCF, CA, and MVM were in charge of processing FTIR spectrometer data. DVI was in charge of numerical



modelling by HYSPLIT. Together DVI, MVM, FH, TB, SCF, CA, VSK, and TW analysed and interpreted the results. DVI, MVM, and VSK prepared the original draft of the manuscript. Together DVI, MVM, FH, TB, SCF, CA, VSK, and TW reviewed and edited the manuscript.

375 **Competing interests**

The authors declare that they have no conflict of interest.

Acknowledgements

Two portable FTIR spectrometers EM27/SUN were provided to St. Petersburg State University, Russia, by the owner - Karlsruhe Institute of Technology, Germany, in compliance with the conditions of temporary importation in the frame of the
380 VERIFY project. The procedure of temporary importation of the instruments to Russian Federation was conducted by the University of Bremen, Germany. Ancillary experimental data were acquired using the scientific equipment of "Geomodel" research centre of St. Petersburg State University. The authors acknowledge the participation of Anatoly V. Poberovskii in the field measurement campaigns. The authors gratefully acknowledge the NOAA Air Resources Laboratory (ARL) for the provision of the HYSPLIT transport and dispersion model used in this publication.

385 **Funding**

This activity has received funding from the European Union's Horizon 2020 research and innovation programme under grant agreement No 776810 (VERIFY project). This work was supported by funding from the Helmholtz Association in the framework of MOSES (Modular Observation Solutions for Earth Systems). The development of the COCCON data processing tools were supported by ESA in the framework of the projects COCCON-PROCEEDS and COCCON-
390 PROCEEDS II. The research was supported by Russian Foundation for Basic Research through the project No.18-05-00011

References

- Ahmadov, R., Gerbig, C., Kretschmer, R., Körner, S., Rödenbeck, C., Bousquet, P., and Ramonet, M.: Comparing high resolution WRF-VPRM simulations and two global CO₂ transport models with coastal tower measurements of CO₂, *Biogeosciences*, 6, 807–817, doi:10.5194/bg-6-807-2009, 2009.
- 395 Airparif, Air quality monitoring network: <https://www.airparif.asso.fr/>, last access 20 May 2020.



- Babenhauserheide, A., Hase, F., and Morino, I.: Net CO₂ fossil fuel emissions of Tokyo estimated directly from measurements of the Tsukuba TCCON site and radiosondes, *Atmos. Meas. Tech.*, 13, 2697–2710, <https://doi.org/10.5194/amt-13-2697-2020>, 2020.
- 400 Bergeron, O. and Strachan, I. B.: CO₂ sources and sinks in urban and suburban areas of a northern mid-latitude city, *Atmos. Environ.*, 45, 1564–1573, doi:10.1016/j.atmosenv.2010.12.043, 2011.
- Bovensmann, H., Buchwitz, M., Burrows, J. P., Reuter, M., Krings, T., Gerilowski, K., Schneising, O., Heymann, J., Tretner, A., and Erzinger, J.: A remote sensing technique for global monitoring of power plant CO₂ emissions from space and related applications, *Atmos. Meas. Tech.*, 3, 781–811, doi:10.5194/amt-3-781-2010, 2010.
- 405 Bréon, F. M., Broquet, G., Puygrenier, V., Chevallier, F., Xueref-Remy, I., Ramonet, M., Dieudonné, E., Lopez, M., Schmidt, M., Perrussel, O., and Ciais, P.: An attempt at estimating Paris area CO₂ emissions from atmospheric concentration measurements, *Atmos. Chem. Phys.*, 15, 1707–1724, <https://doi.org/10.5194/acp-15-1707-2015>, 2015.
- Broquet, G., Bréon, F.-M., Renault, E., Buchwitz, M., Reuter, M., Bovensmann, H., Chevallier, F., Wu, L., and Ciais, P.: The potential of satellite spectro-imagery for monitoring CO₂ emissions from large cities, *Atmos. Meas. Tech.*, 11, 681–708, <https://doi.org/10.5194/amt-11-681-2018>, 2018.
- 410 Canadell, J. G., Ciais, P., Dhakal, S., Dolman, H., Friedlingstein, P., Gurney, K. R., Held, A., Jackson, R. B., Le Quéré, C., Malone, E.L., Ojima, D. S., Patwardhan, A., Peters, G. P., and Raupach, M.R.: Interactions of the carbon cycle, human activity, and the climate system: a research portfolio, *Curr. Opin. Environ. Sustain.*, 2, 301–311, doi:10.1016/j.cosust.2010.08.003, 2010.
- 415 Chen, J., Viatte, C., Hedelius, J. K., Jones, T., Franklin, J. E., Parker, H., Gottlieb, E. W., Wennberg, P. O., Dubey, M. K., and Wofsy, S. C.: Differential column measurements using compact solar-tracking spectrometers, *Atmos. Chem. Phys.*, 16, 8479–8498, <https://doi.org/10.5194/acp-16-8479-2016>, 2016.
- Ciais, P., Bousquet, P., Freibauer, A., and Naegler, T.: Horizontal displacement of carbon associated with agriculture and its impacts on atmospheric CO₂, *Global. Biogeochem. Cy.*, 21, Gb2014, doi:10.1029/2006gb002741, 2007.
- 420 Ciais, P., Crisp, D., Gon, H. v. d., Engelen, R., Heimann, M., Janssens-Maenhout, G., Rayner, P., and Scholze, M.: Towards a European Operational Observing System to Monitor Fossil CO₂ emissions – Final Report from the expert group, European Commission, Copernicus Climate Change Service, Report, 2015.
- COCCON (COllaborative Carbon Column Observing Network): <http://www.imk-asf.kit.edu/english/COCCON.php>, last access 20 May 2020.
- 425 Dietrich, F., Chen, J., Voggenreiter, B., Aigner, P., Nachtigall, N., and Reger, B.: Munich permanent urban greenhouse gas column observing network, *Atmos. Meas. Tech. Discuss.*, <https://doi.org/10.5194/amt-2020-300>, in review, 2020.



- Draxler, R. R. and Hess, G.D.: An overview of the HYSPLIT_4 modelling system for trajectories, dispersion, and deposition. *Aust. Meteor. Mag.*, 47, 295-308, 1998.
- Duren, R. M. and Miller, C.E.: Measuring the carbon emissions of megacities. *Nature Climate Change*, Volume 2, Issue 8, pp. 560-562, doi:10.1038/nclimate1629, 2012.
- 430 EDGAR (Emission Database for Global Atmospheric Research): <https://edgar.jrc.ec.europa.eu/overview.php?v=CO2ts1990-2011>, last access 21 November 2019.
- European Parliament News, CO₂ emissions from cars: facts and figures:
<https://www.europarl.europa.eu/news/en/headlines/society/20190313STO31218>, last access 20 May 2020.
- FLUXNET, <https://fluxnet.fluxdata.org/>, last access 20 May 2020.
- 435 Flesch, T., Wilson, J., Harper, L., Crenna, B., Sharpe, R.: Deducing Ground-to-Air Emissions from Observed Trace Gas Concentrations: A Field Trial, *Journal of Applied Meteorology*, 43, 487-502, doi:10.1175/1520-0450, 2004.
- Foka S.Ch., Makarova M.V., Poberovsky A.V., Timofeev Yu.M.: Temporal variations in CO₂, CH₄ and CO concentrations in Saint-Petersburg suburb (Peterhof), *Optika Atmosfery i Okeana*, 32, 10, 860–866, 2019 [in Russian].
- Gisi, M., Hase, F., Dohe, S., Blumenstock, T., Simon, A., and Keens, A.: XCO₂-measurements with a tabletop FTS using solar absorption spectroscopy, *Atmos. Meas. Tech.*, 5, 2969–2980, <https://doi.org/10.5194/amt-5-2969-2012>, 2012.
- 440 Göckede, M., Michalak, A. M., Vickers, D., Turner, D. P., and Law, B. E.: Atmospheric inverse modeling to constrain regional-scale CO₂ budgets at high spatial and temporal resolution, *J. Geophys.Res.-Atmos.*, 115, D15113, doi:10.1029/2009JD012257, 2010.
- Gurney, K. R., Law, R. M., Denning, A. S., Rayner, P. J., Baker, D., Bousquet, P., Bruhwiler, L., Chen, Y. H., Ciais, P., Fan, S., Fung, I. Y., Gloor, M., Heimann, M., Higuchi, K., John, J., Maki, T., Maksyutov, S., Masarie, K., Peylin, P., Prather, M., Pak, B. C., Randerson, J., Sarmiento, J., Taguchi, S., Takahashi, T., and Yuen, C. W.: Towards robust regional estimates of CO₂ sources and sinks using atmospheric transport models, *Nature*, 415, 626–630, doi:10.1038/415626a, 2002.
- Hase, F., Frey, M., Blumenstock, T., Groß, J., Kiel, M., Kohlhepp, R., Mengistu Tsidu, G., Schäfer, K., Sha, M. K., and Orphal, J.: Application of portable FTIR spectrometers for detecting greenhouse gas emissions of the major city Berlin, *Atmos. Meas. Tech.*, 8, 3059–3068, <https://doi.org/10.5194/amt-8-3059-2015>, 2015.
- Hedelius, J. K., Viatte, C., Wunch, D., Roehl, C. M., Toon, G. C., Chen, J., Jones, T., Wofsy, S. C., Franklin, J. E., Parker, H., Dubey, M. K., and Wennberg, P. O.: Assessment of errors and biases in retrievals of XCO₂, XCH₄, XCO, and XN₂O from a 0.5 cm⁻¹ resolution solar-viewing spectrometer, *Atmos. Meas. Tech.*, 9, 3527–3546, 455 <https://doi.org/10.5194/amt-9-3527-2016>, 2016.



- Hiller, R. V., Neiningner, B., Brunner, D., Gerbig, C., Bretscher, D., Künzle, T., Buchmann, N., and Eugster, W.: Aircraft-based CH₄ flux estimates for validation of emissions from an agriculturally dominated area in Switzerland, *J. Geophys. Res. Atmos.*, 119, 4874–4887, doi:10.1002/2013JD020918, 2014.
- ICOS (Integrated Carbon Observation System): <https://www.icos-ri.eu>, last access 20 May 2020.
- 460 IG3IS (Integrated Global Greenhouse Gas Information System): <https://ig3is.wmo.int/en>, last access 28 May 2020.
- Ionov, D.V. and Poberovskii A.V.: Observations of urban NO_x plume dispersion using the mobile and satellite DOAS measurements around the megacity of St. Petersburg (Russia), *Int. J. Remote Sensing*, 40, 719–733, <https://doi.org/10.1080/01431161.2018.1519274>, 2019.
- Klappenbach, F., Bertleff, M., Kostinek, J., Hase, F., Blumenstock, T., Agusti-Panareda, A., Razinger, M., and Butz, A.:
465 Accurate mobile remote sensing of XCO₂ and XCH₄ latitudinal transects from aboard a research vessel, *Atmos. Meas. Tech.*, 8, 5023–5038, <https://doi.org/10.5194/amt-8-5023-2015>, 2015.
- Koukouli, M.-E., Skoulidou, I., Karavias, A., Parcharidis, I., Balis, D., Manders, A., Segers, A., Eskes, H., and van Geffen, J.: Sudden changes in nitrogen dioxide emissions over Greece due to lockdown after the outbreak of COVID-19, *Atmos. Chem. Phys. Discuss.*, <https://doi.org/10.5194/acp-2020-600>, in review, 2020.
- 470 Kuhlmann, G., Broquet, G., Marshall, J., Clément, V., Löscher, A., Meijer, Y., and Brunner, D.: Detectability of CO₂ emission plumes of cities and power plants with the Copernicus Anthropogenic CO₂ Monitoring (CO₂M) mission, *Atmos. Meas. Tech.*, 12, 6695–6719, <https://doi.org/10.5194/amt-12-6695-2019>, 2019.
- Levin, I., Hammer, S., Eichelmann, E., and Vogel, F. R.: Verification of greenhouse gas emission reductions: the prospect of atmospheric monitoring in polluted areas., *Philos. T. Roy. Soc. A*, 369, 1906–1924, doi:10.1098/rsta.2010.0249, 2011.
- 475 Lopez, M., Schmidt, M., Delmotte, M., Colomb, A., Gros, V., Janssen, C., Lehman, S. J., Mondelain, D., Perrussel, O., Ramonet, M., Xueref-Remy, I., and Bousquet, P.: CO, NO_x and ¹³CO₂ as tracers for fossil fuel CO₂: results from a pilot study in Paris during winter 2010, *Atmos. Chem. Phys.*, 13, 7343–7358, <https://doi.org/10.5194/acp-13-7343-2013>, 2013.
- Makarova, M.V., Arabadzhyan, D.K., Foka, S.C., Paramonova, N.N., Poberovskii, A.V., Timofeev, Yu.M., Pankratova, N.V., and Rakitin, V.S.: Estimation of Nocturnal Area Fluxes of Carbon Cycle Gases in Saint Petersburg Suburbs, *Russ. Meteorol. Hydrol.*, 43, 449–455, <https://doi.org/10.3103/S106837391807004X>, 2018
- 480 Makarova, M. V., Alberti, C., Ionov, D. V., Hase, F., Foka, S. C., Blumenstock, T., Warneke, T., Virolainen, Y., Kostsov, V., Frey, M., Poberovskii, A. V., Timofeyev, Y. M., Paramonova, N., Volkova, K. A., Zaitsev, N. A., Biryukov, E. Y., Osipov, S. I., Makarov, B. K., Polyakov, A. V., Ivakhov, V. M., Imhasin, H. Kh., and Mikhailov, E. F.: Emission



- 485 Monitoring Mobile Experiment (EMME): an overview and first results of the St. Petersburg megacity campaign-2019, *Atmos. Meas. Tech. Discuss.*, <https://doi.org/10.5194/amt-2020-87>, in review, 2020.
- Mays, K. L., Shepson, P. B., Stirm, B. H., Karion, A., Sweeney, C., and Gurney, K. R.: Aircraft-based measurements of the carbon footprint of Indianapolis, *Environ. Sci. Technol.*, 43, 7816–7823, doi:10.1021/es901326b, 2009.
- 490 Nassar, R., Napier-Linton, L., Gurney, K. R., Andres, R. J., Oda, T., Vogel, F. R., and Deng, F.: Improving the temporal and spatial distribution of CO₂ emissions from global fossil fuel emission data sets, *J. Geophys. Res.-Atmos.*, 118, 917–933, <https://doi.org/10.1029/2012JD018196>, 2013.
- NOAA ESRL (Earth System Research Laboratories): <https://www.esrl.noaa.gov/>, last access 20 May 2020.
- NCEP GDAS half-degree archive (National Centers for Environmental Prediction Global Forecast System): <http://www.ndaccdemo.org/>, last access 10 June 2020.
- 495 Oda, T. and Maksyutov, S.: A very high-resolution (1 km×1 km) global fossil fuel CO₂ emission inventory derived using a point source database and satellite observations of nighttime lights, *Atmos. Chem. Phys.*, 11, 543–556, <https://doi.org/10.5194/acp-11-543-2011>, 2011.
- Oda, T. and Maksyutov, S., ODIAC Fossil Fuel CO₂ Emissions Dataset (Version name: ODIAC2019), Center for Global Environmental Research, National Institute for Environmental Studies, doi:10.17595/20170411.001.
- 500 <http://www.nies.go.jp/doi/10.17595/20170411.001-e.html>, last access 1 May 2020.
- Oda, T., Maksyutov, S., and Andres, R. J.: The Open-source Data Inventory for Anthropogenic CO₂, version 2016 (ODIAC2016): a global monthly fossil fuel CO₂ gridded emissions data product for tracer transport simulations and surface flux inversions, *Earth Syst. Sci. Data*, doi:10.5194/essd-10-87-2018, 2018.
- 505 Pacala, S. W., Breidenich, C., Brewer, P. G., Fung, I., Gunson, M. R., Heddle, G., Law, B., Marland, G., Paustian, K., Prather, M., Randerson, J. T., Tans, P., Wofsy, S. C., Linn, A. M., Sturdivant, J., and Al., E.: Verifying Greenhouse Gas Emissions: Methods to Support International Climate Agreements, The National Academies Press, available at: <http://www.nap.edu/catalog/12883.html>, 2010.
- Pathakoti, M., Muppalla, A., Hazra, S., Dangeti, M., Shekhar, R., Jella, S., Mullapudi, S. S., Andugulapati, P., and Vijayasundaram, U.: An assessment of the impact of a nation-wide lockdown on air pollution – a remote sensing perspective over India, *Atmos. Chem. Phys. Discuss.*, <https://doi.org/10.5194/acp-2020-621>, in review, 2020.
- 510 Petetin, H., Bowdalo, D., Soret, A., Guevara, M., Jorba, O., Serradell, K., and Pérez García-Pando, C.: Meteorology-normalized impact of COVID-19 lockdown upon NO₂ pollution in Spain, *Atmos. Chem. Phys. Discuss.*, <https://doi.org/10.5194/acp-2020-446>, in review, 2020.



- Pillai, D., Gerbig, C., Ahmadov, R., Rödenbeck, C., Kretschmer, R., Koch, T., Thompson, R., Neining, B., and Lavrié, J. V.: High-resolution simulations of atmospheric CO₂ over complex terrain – representing the Ochsenkopf mountain tall tower, *Atmos. Chem. Phys.*, 11, 7445–7464, doi:10.5194/acp-11-7445-2011, 2011.
- Pillai, D., Gerbig, C., Kretschmer, R., Beck, V., Karstens, U., Neining, B., and Heimann, M.: Comparing Lagrangian and Eulerian models for CO₂ transport – a step towards Bayesian inverse modeling using WRF/STILT-VPRM, *Atmos. Chem. Phys.*, 12, 8979–8991, doi:10.5194/acp-12-8979-2012, 2012.
- 520 Pillai, D., Buchwitz, M., Gerbig, C., Koch, T., Reuter, M., Bovensmann, H., Marshall, J., and Burrows, J. P.: Tracking city CO₂ emissions from space using a high-resolution inverse modelling approach: a case study for Berlin, Germany, *Atmos. Chem. Phys.*, 16, 9591–9610, <https://doi.org/10.5194/acp-16-9591-2016>, 2016.
- Prairie, Y. T. and Duarte, C. M.: Direct and indirect metabolic CO₂ release by humanity, *Biogeosciences*, 4, 215–217, doi:10.5194/bg-4-215-2007, 2007.
- 525 Roest G.S., Gurney K.R., Miller S.M., Liang J.: Informing urban climate planning with high resolution data: the Hestia fossil fuel CO₂ emissions for Baltimore, Maryland, *Carbon Balance and Management*, under review, doi: <https://doi.org/10.21203/rs.3.rs-16517/v2>, 2020.
- Serebriksky, I.A., (Ed.): The Report on Environmental Conditions in St. Petersburg for 2017, https://www.gov.spb.ru/static/writable/ckeditor/uploads/2018/06/29/Doklad_EKOLOGIA2018.pdf, 2018 (in Russian).
- 530 Serebriksky, I.A., (Ed.): The Report on Environmental Conditions in St. Petersburg for 2018, https://www.gov.spb.ru/static/writable/ckeditor/uploads/2019/08/12/42/doklad_za_2018_EKOLOGIA2019.pdf, 2019 (in Russian).
- Silva, S. J., Arellano, A. F., and Worden, H. M: Toward anthropogenic combustion emission constraints from space-based analysis of urban CO₂/CO sensitivity, *Geophys. Res. Lett.*, 40, 4971–4976, 2013.
- 535 Solodilov V.V. Analytical note “Transport and communication basis for the coordinated development of Moscow and St. Petersburg”, http://www.csr-nw.ru/files/csr/file_category_317.pdf, 2005 (in Russian).
- Stanley, K. M., A. Grant, S. O’Doherty, D. Young, A.J. Manning, A.R. Stavert, T.G. Spain, P.K. Salameh, C.M. Harth, P.G. Simmonds, W.T. Sturges, D.E. Oram and R.G. Derwent, 2018: Greenhouse gas measurements from a UK network of tall towers: Technical description and first results. *Atmospheric Measurement Techniques*, 11(3):1437–1458.
- 540 Stein, A.F., Draxler, R.R., Rolph, G.D., Stunder, B.J.B., and Cohen, M.D., Ngan F.: NOAA’s HYSPLIT atmospheric transport and dispersion modeling system, *Bull. Amer. Meteor. Soc.*, 96, 2059–2077, <http://dx.doi.org/10.1175/BAMS-D-14-00110.1>, 2015.
- TCCON: Total Carbon Column Observing Network, <http://tcon.caltech.edu/>, last access 20 May 2020.



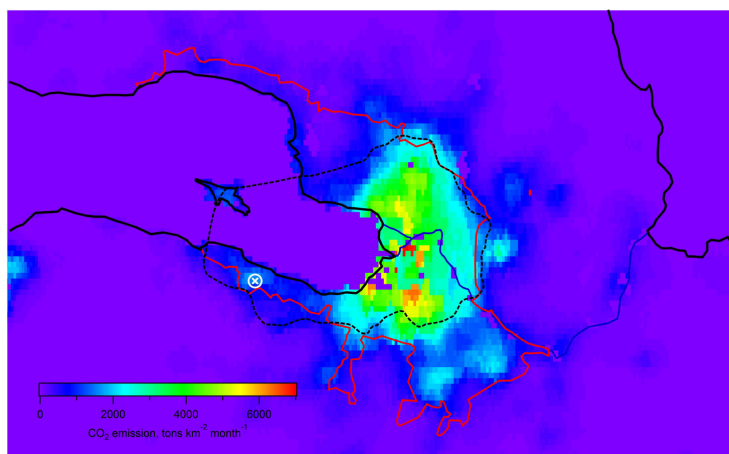
- Turnbull, J., Sweeney, C., Karion, A., Newberger, T., Tans, P., Lehman, S., Davis, K. J., Miles, N. L., Richardson, S. J.,
545 Lauvaux, T., Cambaliza, M. O., Shepson, P., Gurney, K., Patarasuk, R., Zondervan, A.: Towards quantification and
source sector identification of fossil fuel CO₂ emissions from an urban area: Results from the INFLUX experiment, *J.*
Geophys. Res.-Atmos., 120, 292–312, doi:10.1002/2014JD022555, 2014.
- Umezawa, T., Matsueda, H., Oda, T., Higuchi, K., Sawa, Y., Machida, T., Niwa, Y., Maksyutov, S.: Statistical
550 characterization of urban CO₂ emission signals observed by commercial airliner measurements, *Nature, Scientific*
Reports, 10:7963, <https://doi.org/10.1038/s41598-020-64769-9>, 2020.
- UNFCCC: Paris Agreement, FCCC/CP/2015/L.9/Rev1, <http://unfccc.int/resource/docs/2015/cop21/eng/l09r01.pdf>, last
access 20 May 2020, 2015.
- Vogel, F. R., Frey, M., Staufner, J., Hase, F., Broquet, G., Xueref-Remy, I., Chevallier, F., Ciais, P., Sha, M. K., Chelin, P.,
555 Jeseck, P., Janssen, C., Té, Y., Groß, J., Blumenstock, T., Tu, Q., and Orphal, J.: XCO₂ in an emission hot-spot
region: the COCCON Paris campaign 2015, *Atmos. Chem. Phys.*, 19, 3271–3285, [https://doi.org/10.5194/acp-19-](https://doi.org/10.5194/acp-19-3271-2019)
3271-2019, 2019.
- Widory, D. and Javoy, M.: The carbon isotope composition of atmospheric CO₂ in Paris, *Earth Planet. Sc. Lett.*, 215, 289–
298, doi:10.1016/S0012-821x(03)00397-2, 2003.
- WMO Greenhouse Gas Bulletin, 22 November 2018, 14, 1-8, https://library.wmo.int/doc_num.php?explnum_id=5455, last
560 access 21 May 2020, 2018.
- Wunch, D., Wennberg, P. O., Toon, G. C., Keppel-Aleks, G., and Yavin, Y. G.: Emissions of greenhouse gases from a North
American megacity, *Geophys. Res. Lett.*, 36, L15810, <https://doi.org/10.1029/2009GL039825>, 2009.
- Zimnoch, M., Godłowska, J., Necki, J. M., Rozanski, K.: Assessing surface fluxes of CO₂ and CH₄ in urban environment: a
565 reconnaissance study in Krakow, Southern Poland, *Tellus*, 62B, 573-580, [https://doi.org/10.1111/j.1600-](https://doi.org/10.1111/j.1600-0889.2010.00489.x)
0889.2010.00489.x, 2010.
- Zinchenko, A. V., Paramonova, N. N., Privalov, V. I., and Reshetnikov, A. I.: Estimation of Methane Emissions in the St.
Petersburg, Russia, Region: An Atmospheric Nocturnal Boundary Layer Budget Approach, *J. Geophys. Res.*, D20,
107, 2002.



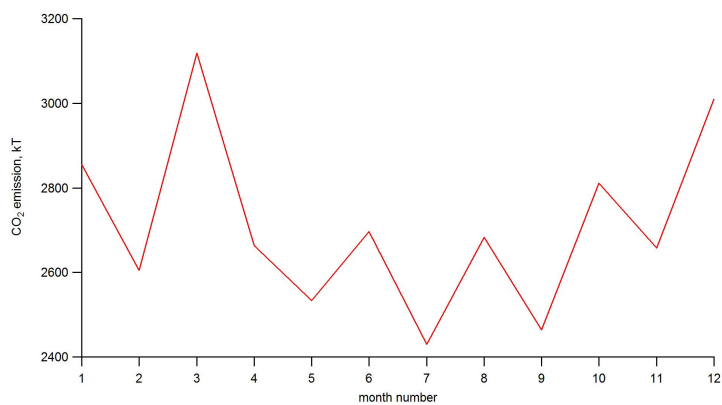
Table 1: The CO₂ area fluxes (kt yr⁻¹ km⁻²) obtained from mobile FTIR measurements in 2019 and 2020 which were performed under similar observational configurations.

Measurement date	CO ₂ area flux [kt yr ⁻¹ km ⁻²]
27/03/2019	76±60
05/04/2020	116±92
01/04/2019	48±38
08/04/2020	89±70

5

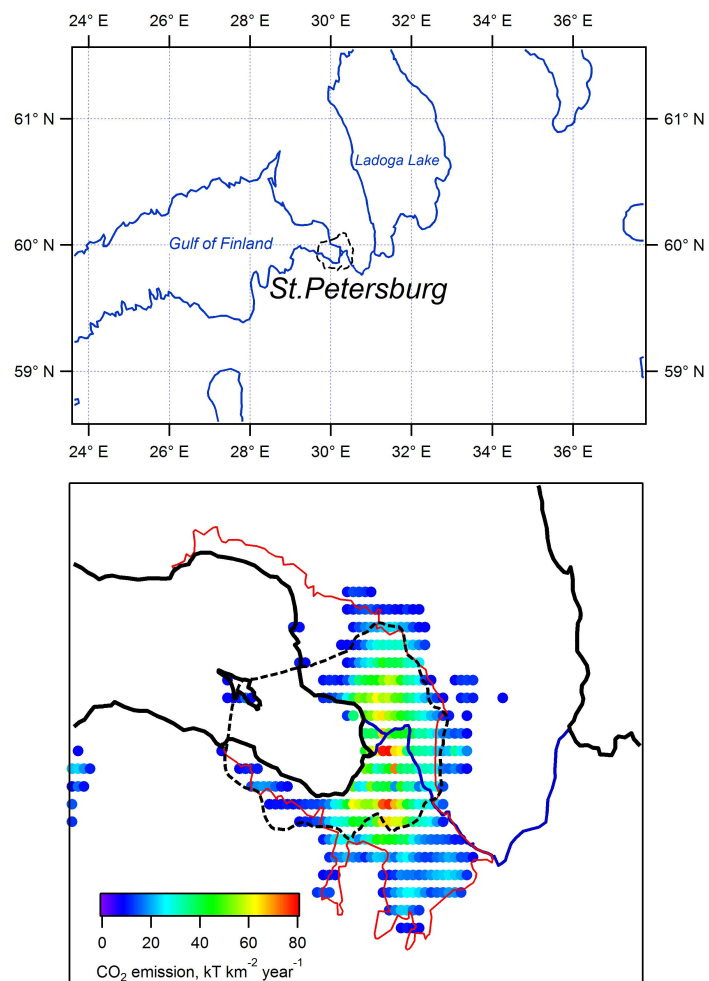


10 **Figure 1:** Spatial distribution of anthropogenic CO₂ emission intensity on the territory of the St. Petersburg agglomeration (59.60-60.29° N, 29.05-31.33° E) according to ODIAC2019 data for April 2018. The red line indicates the administrative border of the city; the black dotted line indicates the city ring road. A white circle depicts the location atmospheric monitoring station of St. Petersburg University in Peterhof (see the text).



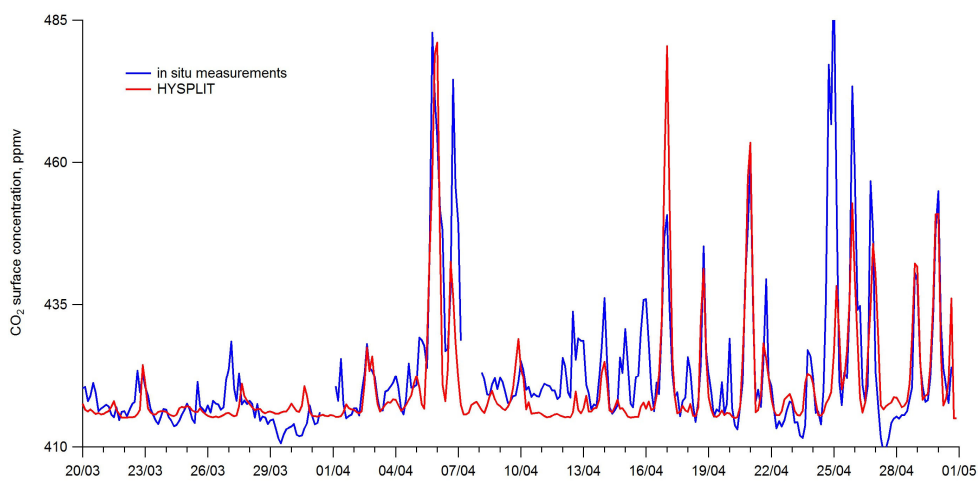
15

Figure 2: Integrated monthly mean FF CO₂ emission from the territory of St. Petersburg according to ODIAC2019 data in 2018.



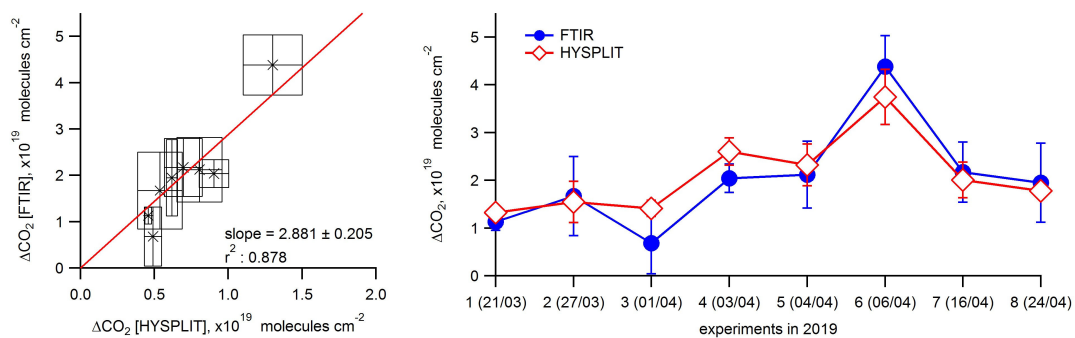
20

Figure 3: Top panel: Map of the spatial domain specified in the HYSPLIT model configuration – the city of St. Petersburg and the surrounding area (top image). Bottom panel: The pixel map of the CO₂ emissions generated using ODIAC2019.



25

Figure 4: Comparison of the HYSPLIT simulations and the in situ measurements of surface CO₂ concentration in Peterhof (59.88° N, 29.82° E) in March-April 2019. Measurement and simulation data are averaged over 3-hour intervals.



30

Figure 5: Left panel: The values of ΔCO_2 (see text) acquired during the field FTIR observations in 2019 compared with the results of HYSPLIT simulations before scaling of the ODIAC data. Measurement and simulation data are averaged over time intervals of FTIR measurements. Right panel: HYSPLIT data obtained using scaled ODIAC CO_2 emissions compared with observed ΔCO_2 . Dots are connected by lines for illustrative purposes only.



35

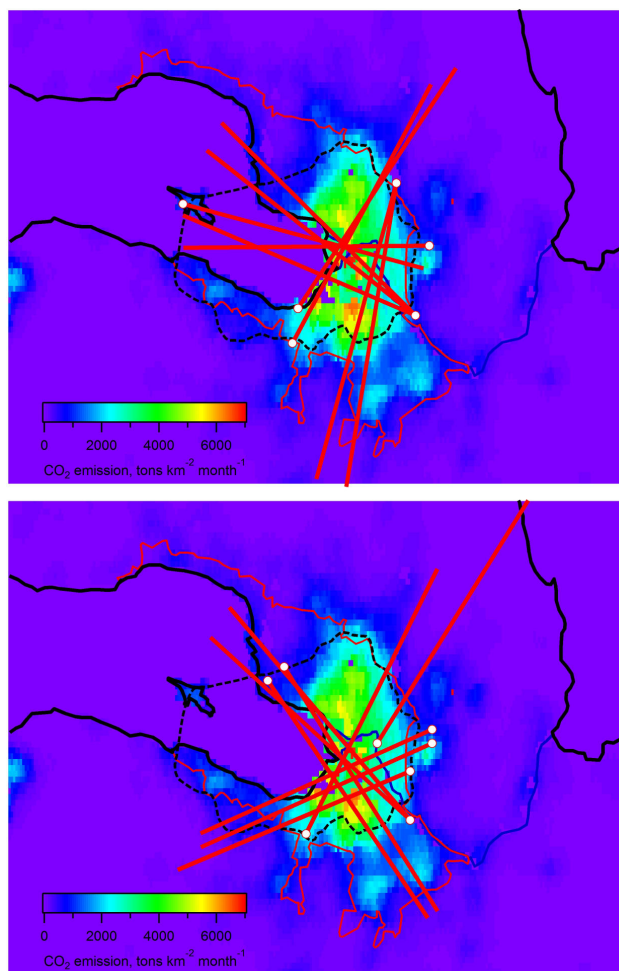
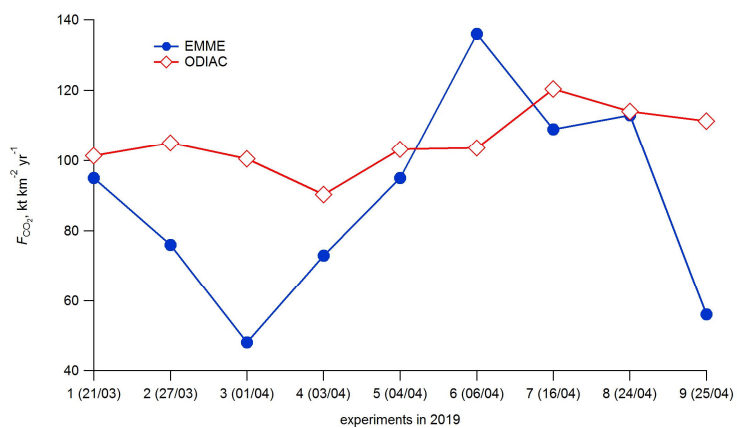
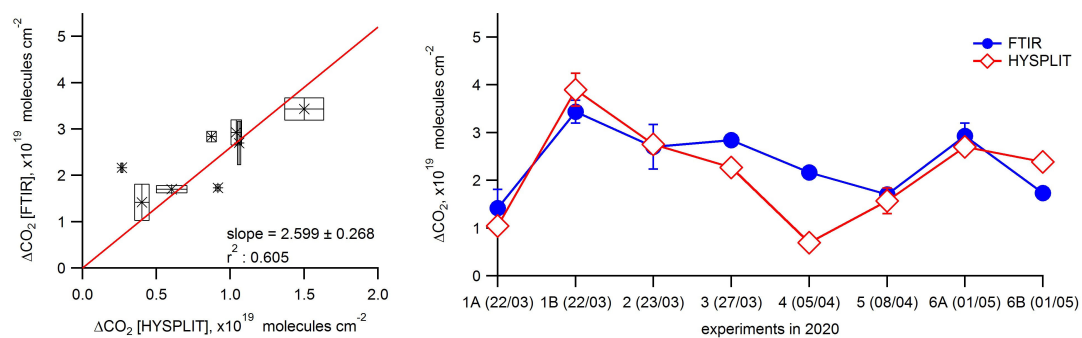


Figure 6: Map of air mass trajectories corresponding to field measurements of EMME experiments in March-April 2019 (top) and March-April 2020 (bottom). For simplicity, the trajectories are designated by straight lines 50 km long, ending at the locations of downwind FTIR measurements.

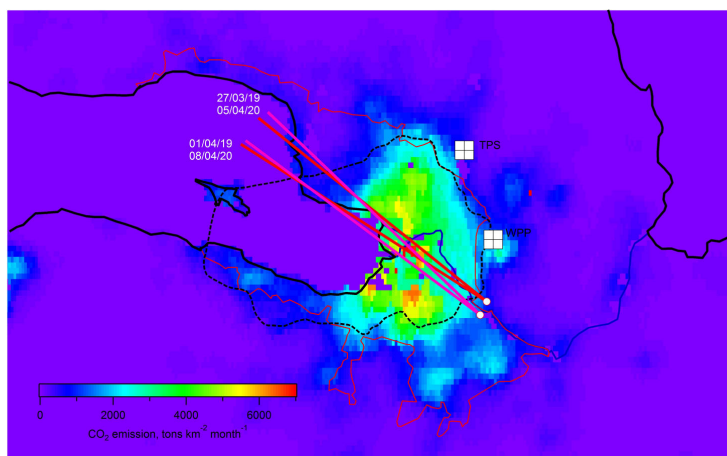
40



45 **Figure 7:** The CO_2 area flux (F_{CO_2}) obtained on the basis of the mass balance approach (EMME-2019) compared to the CO_2 area flux derived from scaled ODIAC data. The calculations are made for the trajectories shown in Fig. 6. Dots are connected by lines for illustrative purposes only.



50 **Figure 8:** Left panel: The values of ΔCO_2 (see text) acquired during the field FTIR observations in 2020 compared with the results of HYSPLIT simulations before the process of scaling of the ODIAC data. Measurement and simulation data are averaged over time intervals of FTIR measurements. Right panel: HYSPLIT data obtained using scaled ODIAC CO₂ emissions compared with observed ΔCO_2 . Dots are connected by lines for illustrative purposes only.



55

Figure 9: Map of similar air trajectories and similar downwind measurement locations for EMME-2019/2020 experiments. For simplicity, the trajectories are marked with straight lines 50 km long, ending at the locations of downwind FTIR measurements. The locations of a thermal power station (TPS) on the north-eastern side and a solid waste processing plant (WPP) on the eastern side are also indicated.

60